HHS Public Access

Author manuscript

Neurobiol Dis. Author manuscript; available in PMC 2017 July 01.

Published in final edited form as:

Neurobiol Dis. 2016 July ; 91: 37–46. doi:10.1016/j.nbd.2016.02.020.

Omega-3 polyunsaturated fatty acids mitigate blood-brain barrier disruption after hypoxic-ischemic brain injury

Wenting Zhang[1,2,*], **Hui Zhang**[1,*], **Hongfeng Mu**[1], **Wen Zhu**[2], **Xiaoyan Jiang**[1,2], **Xiaoming Hu**[1,2], **Yejie Shi**[2], **Rehana K. Leak**[3], **Qiang Dong**[1], **Jun Chen**[1,2,4], and **Yanqin Gao**[1,2]

[1]State Key Laboratory of Medical Neurobiology, Institute of Brain Sciences, Collaborative Innovation Center for Brain Science, and Department of Neurology of Huashan Hospital, Fudan University, Shanghai 200032, China

[2]Center of Cerebrovascular Disease Research and Department of Neurology, University of Pittsburgh School of Medicine, Pittsburgh, PA 15213, USA

[3]Division of Pharmaceutical Sciences, Mylan School of Pharmacy, Duquesne University, Pittsburgh, PA 15282, USA

[4]Geriatric Research, Education and Clinical Center, Veterans Affairs Pittsburgh Health Care System, Pittsburgh, PA 15261, USA

Abstract

Omega-3 polyunsaturated fatty acids (n-3 PUFAs) have been shown to protect the neonatal brain against hypoxic/ischemic (H/I) injury. However, the mechanism of n-3 PUFA-afforded neuroprotection is not well understood. One major determinant of H/I vulnerability is the permeability of the blood-brain barrier (BBB). Therefore, we examined the effects of n-3 PUFAs on BBB integrity after neonatal H/I. Female rats were fed a diet with or without n-3 PUFA enrichment from day 2 of pregnancy to 14 days after parturition. H/I was introduced in 7 day-old offspring. We observed relatively rapid BBB penetration of the small molecule cadaverine (640Da) at 4h post-H/I and a delayed penetration of larger dextrans (3kD–40kD) 24–48h after injury. Surprisingly, the neonatal BBB was impermeable to Evans Blue or 70kD dextran leakage for up to 48h post-H/I, despite evidence of IgG extravasation at this time. As expected, n-3 PUFAs ameliorated H/I-induced BBB damage, as shown by reductions in tracer efflux and IgG

Address correspondence to: Dr. Jun Chen, Center of Cerebrovascular Disease Research, University of Pittsburgh School of Medicine, S507 Biomedical Science Tower, 3500 Terrace Street, Pittsburgh, PA 15213, USA, Tel: +1 (412) 648-1263, chenj2@upmc.edu Or Dr. Yanqin Gao, State Key Laboratory of Medical Neurobiology, Fudan University, Shanghai 200032, China, yqgao@shmu.edu.cn.

*These authors contributed equally to this work.

Author contribution statement

HZ performed all Western blot and gelatin zymography experiments. WZ performed animal surgery. HZ and WZ performed immunohistochemical staining and *in site* zymography staining. HM, YS and XJ did statistical analysis and data interpretation. HZ, WZ (Zhang), WZ (Zhu), XH, RKL and QD wrote the manuscript. YQ and JC designed the study, interpreted the data, and edited the manuscript.

Disclosures/Conflict of interest

The authors declare no conflict of interest.

extravasation, preservation of BBB ultrastructure, and enhanced tight junction protein expression. Furthermore, n-3 PUFAs prevented the elevation in matrix metalloproteinase (MMP) activity in the brain and blood after H/I. Thus, n-3 PUFAs may protect neonates against BBB damage by blunting MMPs activation after H/I.

Keywords

hypoxia/ischemia; blood brain barrier; MMP-9; MMP-2; tight junction

Introduction

Neonatal hypoxic-ischemic (H/I) brain injury is a catastrophic event with high morbidity and mortality. H/I injury may lead to long-term, irreversible neurological and cognitive deficits, including cerebral palsy, epilepsy, and neurodevelopmental disorders. To date, hypothermia is the only therapy showing promise in alleviating functional deficits in H/I patients (Srinivasakumar et al., 2013). Therefore, investigations of the pathological mechanisms underlying neonatal H/I brain injury and the identification of novel, safe therapies for neonates are urgently needed.

The blood brain barrier (BBB) is a large, dynamic structure that is evolutionarily designed to protect the vulnerable brain against blood-borne substances. The BBB is formed early in development and is essential for establishing a stable favorable microenvironment and facilitating nutritional support for cells in the central nervous system during brain maturation. The BBB is comprised of cerebral blood endothelial cells, pericytes, astrocytes, and highly restrictive tight junctions, all of which work in unison to form a robust physical barrier at the dynamic interface between blood, cerebrospinal fluid, and brain. Disruption of this barrier is known to lead to abnormalities in development and neurological function (Ek et al., 2015). However, the differential impact of ischemic injury on the neonatal versus adult BBB remains poorly understood. Early studies reported that the BBB in the developing brain is more vulnerable to ischemic challenges than in the mature brain (Muramatsu et al., 1997). However, recent evidence suggests that the BBB in neonates exhibits greater integrity after H/I injury than in the adult (Fernandez-Lopez et al., 2012). In both neonatal and adult models of stroke, BBB preservation is known to protect the brain against ischemic insults (Chen et al., 2009; Krueger et al., 2015; Li et al., 2013b). Thus, it is important to identify therapies that will preserve BBB integrity in the face of ischemic insults in both the developing and mature brain.

n-3 polyunsaturated fatty acids (PUFAs) are neurotrophic factors known for their beneficial roles in neurodevelopment. Previous research has shown that high levels of n-3 PUFAs protect both the adult and neonatal brain against ischemic brain damage *via* multiple mechanisms, including suppression of inflammatory responses and oxidative stress, enhancement of neurovascular unit reconstruction, and promotion of oligodendrogenesis (Chang et al., 2013; Chen et al., 2014; Hong et al., 2014; Wang et al., 2014; Zhang et al., 2014; Zhang et al., 2015). Recently, Hong *et al.* suggested that docosahexaenoic acid (DHA), the major n-3 PUFA in the brain, protects against BBB disruption after focal

cerebral ischemia in adult rats (Hong et al., 2015). However, it is still unknown whether n-3 PUFAs can preserve BBB integrity following neonatal H/I brain injury.

Matrix metalloproteinases (MMPs) are a family of proteases that participate in physiological and pathophysiological processes, including at the BBB interface. Once activated, MMPs disrupt the BBB by degrading tight junctions and basal lamina proteins, leading to BBB leakage and brain edema. Early application of GM6001, a broad spectrum MMP inhibitor, soon after neonatal H/I brain damage reduces tight junction protein degradation and brain edema, thereby preserving the integrity of the young BBB (Chen et al., 2009). Furthermore, knockout of the MMP-9 gene significantly decreases IgG accumulation in the parenchyma 24 hours after neonatal H/I (Svedin et al., 2007), suggesting that MMP-9 contributes to the early BBB opening (Moretti et al., 2015). Therefore, the present study characterized the impact of n-3 PUFAs on MMP protein and activity levels in both the plasma and the brain.

In the present study, we demonstrate for the first time that n-3 PUFA treatment protects the integrity of the neonatal BBB against H/I injury. Furthermore, our results support the view that inhibition of MMP production and activity might mediate the preservation of the BBB after n-3 PUFA treatment.

Material and Methods

n-3 PUFA dietary enrichment and model of neonatal H/I brain injury

Animal experiments were approved by the Institutional Animal Care and Use Committee at Fudan University, and all procedures were strictly conformed to the *National Institutes of Health Guide for the Care and Use of Laboratory Animals* and ARRIVE (Animal Research: Reporting In Vivo Experiments) guidelines. Timed pregnant female Sprague-Dawley rats (Shanghai SLAC Laboratory Animal Co. Ltd. Shanghai, China) were randomly assigned to be fed a regular laboratory rodent diet with an inherently low n-3 PUFAs concentration (0.5%; N3L) or the same diet supplemented with n-3 PUFAs [N3H; DHA and eicosapentaenoic acid (EPA), Puritan's Pride, Oakdale, USA; final n-3 PUFAs concentration 1.5%] from the second day of pregnancy to 14 days after parturition. DHA and EPA contents were 60 and 90 mg, respectively, in every gram of N3H diet. Seven day-old rat pups were then subjected to H/I brain injury as previously described (Zhang et al., 2010). Briefly, the left common carotid artery was ligated under anesthesia with 3% isoflurane. After a 1.5-hour recovery period, the pups were placed in a chamber containing a humidified atmosphere of 8% O_2/92% N_2 for 2.5 hours and then returned to their dams. The overall mortality rate in the N3L H/I group was 8.4%, whereas it was 1.3% in the N3H H/I group. The majority of death in either groups occurred during or shortly after the hypoxic procedure, the dead animals were excluded from any further experiments or data analysis. In the sham surgery group, a ligature was placed loosely around the left common carotid artery but not ligated, and the pups were not subjected to hypoxia.

Brain water content measurement

Animals were sacrificed under deep anesthesia with 3% isoflurane at 48 hours after H/I. The brain was harvested and dissected along the sagittal fissure into ipsilateral and contralateral

hemispheres. Total wet weight was measured immediately and the brain was then heated to 100°C in a drying oven for 72 hours before measuring the dry weight (wet and dry weights were accurate to 0.1 mg). The percentage brain water content in each hemisphere was calculated with the following equation: ((wet weight − dry weight) / wet weight) × 100%.

Intravenous injection, detection, and quantification of tracers

Cadaverine Alexa-488 (640Da; 200μg/pup, Invitrogen, Waltham, USA) or dextran of various molecular weights (3kD, 40kD and 70kD) was injected intravenously 1, 21, or 45 hours post H/I. Animals were sacrificed 3 hours following tracer infusions, perfused, and fixed with paraformaldehyde. Brains were removed and cut into 25 μm slices. Coronal brain sections were stained with RECA-1 (1:1000, AbD Serotec, Kidlington, UK) to visualize the cerebrovascular system. Fluorescence images were captured and the distribution of tracers was calculated using ImageJ software by a blinded observer.

Evans blue infusions

BBB permeability was determined by measuring Evans blue (EB) extravasation. A solution of 2% EB dye (3mL/kg, Sigma Aldrich, St. Louis, USA) was slowly administered intravenously at 1, 21 and 45 hours after reperfusion onset. Three hours following infusion, animals were perfused with 200 mL saline and decapitated. The brain was dissected into two hemispheres and soaked in methanamide separately for 48 hours. To pellet the brain tissue, the sample was centrifuged for 30 minutes at 14,000 rpm. The absorption of the supernatant was measured at 632 nm with a spectrophotometer (Bio-Rad, Hercules, USA). The EB content was calculated as μg/g of brain tissue using a standardized curve by a blinded observer.

Measurement of endogenous immunoglobulin G (IgG) extravasation

The area of extravasation of endogenous IgG molecules was determined by immunohistochemical staining for rat IgGs on 25 μm-thick free-floating coronal brain sections. Sections were blocked with 5% goat serum in phosphate-buffered saline with 0.1% Triton-X 100 for 1 hour, followed by a 2-hr incubation in DyLight™ 488-conjugated goat-anti-rat IgG antibody (1:1000; Jackson ImmunoResearch Laboratories, West Grove, USA) at room temperature. The IgG-positive area was calculated by a blinded observer using ImageJ software. Four animals were analyzed in each group.

Transmission electron microscopy

BBB ultrastructure was detected by transmission electron microscopy at 48 hours after ischemia. Proximal middle cerebral artery cortical tissues were fixed in 2.5% glutaraldehyde in 0.1M phosphate buffer (pH 7.4) for 12 hours and 1% osmium tetroxide for 1 hour. After dehydration in an alcohol series, tissues were embedded in 618# resin. Ultrathin sections were prepared using a Reichert ultramicrotome, contrasted with uranyl acetate and lead citrate, and examined with a Philips CM120 electron microscope (FEI, Hillsboro, USA) at 80kv.

Western blotting

Western blots were performed using the standard SDS-PAGE method as previously described (Zhang et al., 2015). Briefly, PVDF membranes were blocked in 5% non-fat dry milk in Tris-buffered saline with Tween (TBST; 10 mM Tris–HCl, 150 mM NaCl, and 0.1% Tween) for 1 hour at room temperature. Membranes were then incubated overnight at 4°C with rabbit polyclonal antibodies directed against MMP-2 (1:100; Abcam, Cambridge, UK), MMP-9 (1:500; Abcam, Cambridge, UK), collagen IV (1:1000, Abcam, Cambridge, UK), occludin (1:100; Abcam, San Francisco, USA), cadherin-10 (1:1000; Abcam, Cambridge, UK), ZO-1 (1:100, Invitrogen, Waltham, USA), claudin-5 (1:100; Invitrogen, Waltham, USA), and mouse monoclonal antibodies against β-actin (1:5000, Sigma-Aldrich, St. Louis, USA). Goat anti-rabbit IgG (H+L) 800CW, goat anti-rabbit (H+L) 680LT, goat anti-mouse (H+L) 800CW and/or goat anti mouse (H+L) 680LT were then applied for 90 minutes at room temperature (1:5000, LI-COR Bioscience, Lincoln, USA) prior to washing with TBST. Protein bands were visualized with an Odyssey Imager and Odyssey software (LI-COR, Lincoln, USA). In order to detect multiple proteins on a single membrane, the membrane was incubated in restore plus western blot stripping buffer (Pierce Biotechnology, Waltham, USA) for 15 minutes at room temperature between labeling procedures. Protein levels were semi-quantitatively measured by Quantity One 4.5.2 software (Bio-Rad, Hercules, USA). Three independent experiments were performed in duplicate and data were quantified from 6 animals per group.

Gelatin zymography

Zymography was carried out in 8% sodium dodecyl sulfate (SDS)-polyacrylamide gels containing 0.1% gelatin. Protein samples (20μg) were mixed with 2× non-reducing sample buffer (20% glycerol, 2% SDS, 0.04% bromophenol blue) and subjected to electrophoresis in a mini-gel apparatus (Bio-Rad, Hercules, USA). Following electrophoresis, gels were washed twice with 2.5% Triton X-100 for 1 hour to remove the SDS and incubated 40 hours at 37°C in digestion buffer (50 mM Tris–HCl, 50 mM NaCl, 5 mM $CaCl_2$, 2 μM $ZnCl_2$, 0.02% Brij-35, pH 7.6). After incubation, gels were stained for 3 hours with 0.5% Coomassie blue and destained in buffer containing 30% methanol and 10% glacial acetic acid. Bands reflecting gelatinolytic activity were scanned and analyzed by Quantity One software (Bio-Rad, Hercules, USA). Three independent experiments were performed in duplicate.

In situ zymography and double labeling with fluorescent probes

To examine the cellular localization of gelatinolytic activity, *in situ* zymography with double fluorescent staining was performed. Animals were sacrificed 48 hours after H/I and brain were collected and frozen on dry ice. Frozen sections were cut at 15μm using a cryostat. Sections were incubated with 200μg/ml fluorescein-conjugated DQ gelatin (Enzecheck Gelatinase Assay Kit, Invitrogen, Waltham, USA) for 1 hour at 37°C. The sections were then fixed in 4% paraformaldehyde for 30 minutes, and incubated with mouse anti-NeuN (1:500; Millipore, Billerica, USA), rabbit anti-GFAP (1:500; Dako, Carpinteria, USA) and Texas Red-conjugated tomato lectin (1:500; Vector laboratories, Burlingame, USA) for 1 hour at room temperature and overnight at 4°C. Brain sections were then incubated in

DyLight™ 594-conjugated goat anti-rabbit or anti-mouse secondary antibodies (1:1000; Jackson ImmunoResearch Laboratories, West grove, USA) at room temperature for 1 hour. Sections were subsequently mounted and coverslipped with Fluoromount-G (Southern Biotech, Birmingham, USA).

Immunohistochemical staining

Immunohistochemical staining was performed as previously described (Zhang et al., 2015). Briefly, coronal brain sections were blocked with 5% goat serum in phosphate-buffered saline with 0.1% Triton-X 100 for 1 hour, followed by primary antibody incubations for 1 hour at room temperature and overnight incubation at 4°C. The following primary antibodies were used: Rabbit anti-MMP-9 polyclonal antibody (1:100; Abcam, Cambridge, UK), mouse monoclonal anti-NeuN antibody (1:500; Millipore, Billerica, USA), rabbit polyclonal anti-vWF antibody (1:200; Dako, Carpinteria, USA), rabbit polyclonal anti-Iba1 antibody (1:1000, Wako, Richmond, USA), rabbit polyclonal anti-ZO-1 antibody (1:50, Invitrogen, Waltham, USA), rabbit monoclonal anti-claudin-5 antibody (1:100; Invitrogen, Waltham, USA), rabbit polyclonal anti-occludin antibody (1:50; Abcam, Cambridge, UK), mouse monoclonal anti-RECA-1 antibody (1:1000, AbD Serotec, Kidlington, UK), and rabbit polyclonal anti-GFAP antibody (1:500; Dako, Carpinteria, USA). Sections were then washed three times in phosphate-buffered saline, and incubated with fluorophore-conjugated secondary antibodies for 1 hour at room temperature. To visualize $NeuN^+$ neurons, $GFAP^+$ astrocytes, $Iba1^+$ microglia, and vWF^+ endothelial cells, sections were incubated in DyLight™ 488-conjugated goat anti-mouse or goat anti-rabbit secondary antibodies (1:1000; Jackson ImmunoResearch Laboratories, West grove, USA). DyLight™ 594-conjugated goat anti-rabbit and goat anti-rat secondary antibodies (1:1000; Jackson ImmunoResearch Laboratories, West grove, USA) were used to visualize MMP-9 and RECA-1, respectively. Tight junction protein ZO-1, claudin-5, and occludin were labeled with DyLight™ 488-conjugated goat anti-rabbit secondary antibodies. Sections were subsequently washed, mounted and coverslipped with Fluoromount-G (Southern Biotech, Birmingham, USA). Fluorescence images were captured by a blinded observer as described above.

Real-time polymerase chain reaction analysis

Quantitative polymerase chain reaction was performed with the Opticon 2 Real-Time Polymerase Chain Reaction Detection System (Bio-Rad, Hercules, USA) using corresponding primers and the SYBR green Polymerase Chain Reaction Master Mix (Applied Biosystems, Waltham, USA). Reverse-transcribed RNA was amplified by PCR under the following conditions: 95 °C for 5 min, 40 cycles of 30 s at 94 °C, 30 s at 65 °C, 20 s at 72 °C and a final extension step for 10 min at 72 °C. The cycle time values of the genes of interest were first normalized to levels of glyceraldehyde-3-phosphate dehydrogenase (GAPDH) in the same sample and gene expression levels were expressed as fold changes versus sham. Primer sequences used are listed in following: MMP-2, 5’-GATCTGCAAGCAAGACATTGTCTT-3’(forward), 5’-GCCAAATAAACCGATCCTTGAA-3’(reverse); MMP-9, 5’-GTAACCCTGGTCACCGGACTT-3’(forward), 5’-ATACGTTCCCGGCTGATCAG-3’

(reverse); GAPDH, 5'-AACCTGCCAAGTATGATGACATCA-3'(forward), 5'-TGTTGAAGTCACAGGAGACAACCT-3'(reverse).

Statistical Analysis

All data are reported as mean±SEM. Significant differences between means were assessed by analysis of variance and *post hoc* Scheffe tests for multiple comparisons. $P \leq 0.05$ was considered statistically significant.

Results

n-3 PUFA treatment prevents BBB permeability after H/I brain injury

The pathology of H/I brain injury involves disruption of the BBB (Ek et al., 2015), which contributes to cerebral edema and secondary neuronal injury. As a measure of edema, hemispheric water content was examined 48 hours after H/I injury. Compared to sham controls, animals in both normal diet (N3L) and n-3 PUFA-supplemented (N3H) groups showed increased brain water content, indicating significant brain edema following H/I. However, n-3 PUFA treatment significantly reduced water content in the ipsilateral brain tissue (Figure 1A).

To further investigate the effect of n-3 PUFAs on BBB integrity after H/I, we measured the extravasation of fluorescent tracers of various molecular weights, including cadaverine Alexa-488 (640Da) and 3kD, 40kD or 70kD dextran. In animals on a normal diet, leakage of cadaverine out of the vasculature was observed in the ipsilateral cortex and striatum as early as 4 hours after H/I and remained prominent for 48 hours, whereas cadaverine was restricted to vessels in sham-operated animals. As expected, n-3 PUFA treatment significantly reduced cadaverine extravasation in the ipsilateral brain both at 4 hours and 48 hours following H/I (Figure 1B). At 48 hours after H/I injury, the fluorescent intensity of cadaverine within the ischemic core area in the ipsilateral cortex was increased 9.35-fold over sham, and this was dramatically reduced by n-3 PUFA treatment (Figure 1C). Extravasation of 3kD and 40kD dextran into the brain parenchyma was relatively delayed but became prominent at 24 hours after H/I injury (Figure 1D and 1E). Compared to animals on a normal diet, n-3 PUFA-treated animals exhibited lower extravasation of 3kD and 40kD dextrans following H/I. In addition, 70kDa dextran failed to permeate the immature brain even at 48 hours after H/I (Figure 1D).

The EB dye binds to serum albumin (67kD) immediately following intravenous injection and was also used to measure BBB integrity. EB was barely detectable in the ipsilateral hemisphere after H/I injury (Figure 2A), and no significant difference in total EB content was detected between the sham and H/I groups (Figure 2B).

Taken together, these data suggest that neonatal H/I injury induces BBB leakage of molecules less than or equal to 40kD in size, and that n-3 PUFA dietary supplementation reduces this BBB permeability after H/I.

Despite their large molecular weight (~140kD), plasma-derived IgG molecules leaked into the ipsilateral cortex, striatum, and hippocampus in normal diet neonates after the H/I insult,

suggesting that IgGs may traverse the compromised BBB through mechanisms other than paracellular leakage. As expected, n-3 PUFA treatment significantly reduced IgG extravasation after H/I (Figure 3).

n-3 PUFA treatment preserves the integrity of tight junctions after H/I injury

Tight junction proteins are essential for the proper maintenance of BBB integrity. Western blotting experiments revealed that the expression of tight junction proteins, such as occludin, ZO-1, claudin-5, and cadherin-10 was greatly decreased 48 hours after H/I injury and that n-3 PUFA treatment significantly preserved the expression of these proteins (Figures 4A and 4B). Reduction in occludin, claudin-5, and ZO-1 expression in endovascular cells after H/I injury was further confirmed by immunofluorescent staining (Figure 4D). As expected, n-3 PUFA dietary supplementation markedly retained their *in situ* expression.

In order to investigate the effect of n-3 PUFAs on BBB ultrastructure after the H/I insult, transmission electron microscopy was employed. Sham-operated animals exhibited capillary integrity with normal endothelial cells and basal lamina. In N3L H/I brains, endothelial cells became swollen and deformed, and the number of tight junctions was concomitantly decreased (Figure 4C). Furthermore neuronal ultrastructure was severely compromised and neuronal mitochondria were decreased and showed obvious vacuolization (Figure 4C top line). Astrocytic perivascular processes were severely swollen and exhibited reduced electron density. n-3 PUFA-treated H/I brains exhibited profound protection against each of these changes in BBB ultrastructure (Figure 4C). These findings suggest that the integrity of BBB is robustly protected by n-3 PUFA treatment.

n-3 PUFA treatment suppresses MMP-9 and MMP-2 expression in brain parenchyma after neonatal H/I injury

MMPs, especially MMP-2 and MMP-9, play essential roles in the degradation of the extracellular matrix and BBB disruption (Yang and Rosenberg, 2015). In order to determine the effect of n-3 PUFA treatment on MMP production, MMP-2 and MMP-9 expression was measured by Western blotting and immunofluorescent staining at various time points after neonatal H/I injury. Upregulation of MMP-9 and MMP-2 mRNA was detected as early as 4 hours after H/I injury (Figure 5A). Furthermore, MMP-9 mRNA expression remained elevated at 24 hours after H/I. As expected, n-3 PUFA treatment prevented the elevations in MMP-9 and MMP-2 mRNA. Compared to sham controls, MMP-9 protein expression was significantly increased in the brain at 24 and 48 hours after H/I injury (Figure 5B and 5C). The upregulation of MMP-2 protein was relatively delayed until 48 hours after H/I. n-3 PUFA dietary supplementation significantly attenuated H/I-induced upregulation of both of these proteins after H/I (Figures 5B and 5C). Protein expression of collagen IV (Col-IV), the principal collagen type in the neurovascular basal lamina, was significantly reduced at 4, 24, and 48 hours after H/I in the N3L group compared to sham animals. n-3 PUFA treatment restored Col-IV expression at both 24 and 48 hours, but not 4 hours after H/I injury (Figures 5B and 5C).

To further determine the source of MMP-9, immunofluorescent dual-staining of MMP-9 with $NeuN^+$ neurons, $GFAP^+$ astrocytes, $Iba1^+$ microglia, and vWF^+ endothelial cells was

performed at 48 hours after H/I injury. MMP-9 expression was only detected at low levels within neurons of sham-injured brains. After H/I injury, endothelial cells and activated astrocytes increased intracellular MMP-9 expression. Neuronal expression of MMP-9 was also elevated in cells with condensed nuclei. Negligible MMP-9 expression was detected in microglia 48 hours after H/I injury (Figure 5D). n-3 PUFAs significantly inhibited H/I-induced expression of MMP-9 in neurons, astrocytes, and endothelial cells.

n-3 PUFA treatment attenuates H/I-induced activation of MMP-9 and MMP-2 in brain and plasma

In order to verify an effect of n-3 PUFAs on MMP-9 and MMP-2 function, we measured MMP-9 and MMP-2 activities in brain extracts using gelatin zymography at 48 hours after H/I injury. MMP-9 and MMP-2 activities were markedly increased in the H/I brain, and were both significantly attenuated by n-3 PUFA treatment (Figure 6A and 6B). *In situ* zymography was performed using fluorescein-conjugated DQ gelatin. In the sham group, the enzymatic activity of MMPs was low and dispersed mainly in and around neurons in the cerebral cortex at 48 hours after H/I insult (Figure 6C). MMP activity was greatly upregulated in $NeuN^+$ neurons with condensed nuclei in the ipsilateral cortex 48 hours after H/I injury. In addition, activated MMPs were also deposited in and around blood vessels. Notably, negligible MMP activation was observed in astrocytes (Figure 6C), suggesting proteolytic activation of MMP-9 following release from astrocytes (Maddahi et al., 2009; Neuhaus et al., 2014). As expected, n-3 PUFA treatment dramatically suppressed the extensive activation of MMPs in the brain parenchyma at the same time point (Figure 6B and 6C).

Due to the importance of periphery-derived MMPs in BBB disruption (Gidday et al., 2005; Li et al., 2013a), the expression and enzymatic activity of MMP-2 and MMP-9 were also examined in plasma. H/I injury resulted in a pronounced increase of MMP-9 expression in plasma beginning from 1 hour after damage, and this was significantly suppressed by n-3 PUFA treatment (Supplementary Figure 1A, 1B and 1E). Plasma MMP-9 activity was significantly enhanced as early as 1 hour following H/I injury and sustained for 24 hours (Supplementary Figure 1C, 1D and 1E). n-3 PUFA treatment mitigated this prolonged activation in plasma (Supplementary Figure 1E). No significant differences were detected in MMP-2 expression and activity in plasma at 1 or 24 hours after H/I injury (Supplementary Figure 1).

Discussion

The present study demonstrates that dietary supplementation with n-3 PUFAs preserves the integrity of the neonatal BBB following H/I brain injury, perhaps through suppression of central and peripheral MMP activation and of degradation of the extracellular matrix and tight junction proteins.

Experimental models of cerebral ischemia in neonatal rodents have shown that the pathophysiology of perinatal brain damage is quite different from that in the adult. A recent study reported that the BBB was markedly less damaged by acute ischemic stroke in neonatal rats than adult rats, probably due to differential expression of basal lamina and tight

junction proteins and neutrophil behavior (Ek et al., 2015; Fernandez-Lopez et al., 2012; Moretti et al., 2015). In the present study, we characterized BBB integrity after neonatal H/I brain injury. We discovered a rapid increase in BBB permeability to low molecular weight molecules (cadaverine, 640Da) as early as 4 hours after the H/I insult, and a relatively delayed leakage of dextrans (3kD–40kD) 24 hours post-injury. High molecular weight dextran molecules (70kD) and EB remained confined to the circulation by the neonatal BBB up to 48 hours post-injury. These findings are consistent with previous reports that the neonatal BBB is relative impermeable after H/I insults compared to the adult BBB (Fernandez-Lopez et al., 2012). Recent studies further suggest that DHA reduces the infarct area after focal brain injury by mitigating BBB disruption in adult rats (Hong et al., 2015). Herein, we demonstrated that n-3 PUFA treatment also preserved the integrity of the BBB in the developing brain after neonatal H/I injury.

In contrast to high molecular weight dextrans and EB, IgG (~140kD) extravasation was prominent in neonates after H/I injury. It is possible that transcellular rather than paracellular mechanisms contribute to this process. The exact mechanisms underlying IgG leakage following H/I remain unclear. Previous *in vitro* and *in vivo* studies suggest that FcRn and low-density lipoprotein receptor-related protein 1 (LRP-1), both expressed at the BBB, are potential candidates for mediating specific transport of antibodies (Deane et al., 2005; Proulx et al., 2012). For example, FcRn is expressed in microvasculature in the rat brain and mediates the efflux of IgG across the BBB (Zhang and Pardridge, 2001). LRP1, an endocytic receptor involved in transcytosis of several proteins across the BBB, has been shown to facilitate IVIg internalization (Proulx et al., 2012). In human smooth muscle cells, hypoxia induces sustained LRP1 overexpression (Revuelta-Lopez et al., 2013). Thus, H/I may stimulate the expression and redistribution of these two receptors in the neonatal BBB and lead to IgG accumulation in injured brain parenchyma. Of note, recent studies indicate that LRP1 is regulated by the membrane type MMP subfamily and that it modulates expression and activation of MMP-9 in different cell types (Hahn-Dantona et al., 2001; Revuelta-Lopez et al., 2013; Rozanov et al., 2004; Song et al., 2009). Therefore, the aberrant expression and activation of MMPs in neonatal H/I injury may also contribute to IgG extravasation.

One potentially important mechanism whereby n-3 PUFAs protect against neonatal H/I injury may be the modulation of central and peripheral MMP production and activity. MMPs play key roles in basal membrane and tight junction protein degradation and state modulation (Coisne and Engelhardt, 2011), which result in BBB damage and facilitate the accumulation of immune cells in the brain (Labus et al., 2014). In MMP-9-deficient neonatal mice, the leakage of the BBB is diminished, indicating that excessive MMP-9 activation might result in BBB damage after H/I (Svedin et al., 2007). Furthermore, inhibition of MMP-9 may reduce brain edema and BBB disruption by enhancing TJ protein formation and promoting angiogenesis (Yang et al., 2013). Consistent with previous reports, our study shows that mRNA and protein expression of MMP-9 and MMP-2 was significantly enhanced by H/I in neonatal rat brains. As hypothesized, n-3 PUFA treatment markedly reduced the production and activation of MMP-9 and MMP-2. Previous studies indicate that brain microvascular endothelium cells are the major early sources of MMP-9 in the brain soon after focal cerebral ischemia (Jeffery et al., 1987; Jin et al., 2010; McColl et al., 2008). Our findings demonstrate that MMP-9 protein expression was profoundly affected in

neurons and astrocytes after H/I injury. However, MMP enzymatic activity was high in neurons and vessels but not in activated astrocytes after H/I. It is possible that MMP-9 is produced by astrocytes but activated only after release to induce matrix degradation and BBB disruption. We found that MMP-9 expression and activity is elevated as early as 1 hour after H/I injury in the plasma, much earlier than MMP-9 in brain parenchyma, and that this elevation persists up to 24 hours. Studies have shown that the increase in plasma MMP-9 is strongly correlated with the severity of acute cerebrovascular disease and infarct volume, suggesting that therapies targeting plasma MMP-9 may show promise in neonatal H/I (Bednarek et al., 2012). Here, we showed that n-3 PUFAs not only suppressed MMP activation in the brain, but also restricted circulation-derived MMP expression and activity following H/I. This simultaneous inhibition of central and peripheral MMPs may bestow n-3 PUFAs with potent protective effects, as shown by marked preservation of BBB integrity and significant limitation of H/I brain injury in neonatal rats.

The inhibitory effects of n-3 PUFAs on MMPs production from multiple cell types after H/I are consistent with the previously reported effect on MMP-9 production and release from peripheral immune cells (Shinto et al., 2009; Shinto et al., 2011), microglia (Liuzzi et al., 2007) and astrocytes (Petroni et al., 1994). n-3 PUFAs may inhibit inflammation-induced MMP-9 production through direct and indirect mechanisms. n-3 PUFAs have shown the ability to inhibit the DNA binding activity of nuclear factor-kappa B (NF-κB) and activator protein-1 (AP-1), both of which have binding sites on the promoter of the MMP-9 gene (St-Pierre et al., 2003; Zhao and Chen, 2005). Thus, n-3 PUFAs may decrease MMP-9 production by reducing NF-κB- and AP-1-mediated MMP-9 gene transcription. Alternatively, n-3 PUFAs may reduce MMP-9 levels by decreasing the levels of pro-inflammatory cytokines, several of which, such as TNF-α and IL-1β, are potent inducers for MMP-9 production (St-Pierre et al., 2003). The anti-inflammatory effect of n-3 PUFAs is well established (Chen et al., 2014; Zhang et al., 2010). Nevertheless, future studies are warranted to elucidate the precise signaling mechanism by which n-3 PUFAs inhibits MMP-9 expression and activity after HI, as different signaling pathways could be engaged in different cell types under different pro-inflammatory conditions.

Conclusions

In conclusion, the present study is the first to demonstrate that n-3 PUFAs treatment alleviates BBB damage induced by H/I in neonates. Our results also suggest that n-3 PUFA treatment may protect the BBB by inhibiting central and peripheral MMP production and activity. Therefore, high fish product diets or fish oil capsules ingested during pregnancy may help promote neonatal brain health. Further investigation of n-3 PUFAs as prophylactic or therapeutic agents against neonatal H/I brain injury are warranted.

Supplementary Material

Refer to Web version on PubMed Central for supplementary material.

Acknowledgments

Sources of Funding

This project was supported by the Chinese Natural Science Foundation grants 81020108021, 81171149, 81371306 (to Dr Gao), and 81228008 (to Dr Chen); the Shanghai Committee of Science and Technology Support Program 14431907002 (to Dr Gao); the U.S. NIH grants NS095671, NS36736, NS089534 and NS45048 (to Dr Chen); the U.S. Department of Veterans Affairs Research Career Scientist Award and RR & D Merit Review I01RX000420 (to Dr Chen); and the American Heart Association Scientist Development grant 13SDG14570025 (to Dr Hu) and 15POST22260011 (to Dr. Shi). Dr. Wenting Zhang was supported by the Young Teacher Program of Fudan University (No.20520131150), and National Natural Science Foundation grants (No. 81100978 and No. 81471332).

Abbreviations

BBB	blood brain barrier
Col-IV	collagen IV
DHA	docosahexaenoic acid
EPA	eicosapentaenoic acid
EB	evans blue
FcRn	neonatal Fc receptor
GAPDH	glyceraldehyde-3-phosphate dehydrogenase
H/I	hypoxic/ischemic
LRP1	low-density lipoprotein receptor-related protein 1
MMP	matrix metalloproteinase
PUFA	polyunsaturated fatty acids
SDS-PAGE	sodium dodecyl sulfate polyacrylamide gel electrophoresis
TJ	tight junction
vWF	von Willebrand factor

References

Bednarek N, et al. Increased MMP-9 and TIMP-1 in mouse neonatal brain and plasma and in human neonatal plasma after hypoxia-ischemia: a potential marker of neonatal encephalopathy. Pediatr Res. 2012; 71:63–70. [PubMed: 22289852]

Chang CY, et al. Docosahexaenoic acid reduces cellular inflammatory response following permanent focal cerebral ischemia in rats. J Nutr Biochem. 2013; 24:2127–2137. [PubMed: 24139673]

Chen S, et al. n-3 PUFA supplementation benefits microglial responses to myelin pathology. Sci Rep. 2014; 4:7458. [PubMed: 25500548]

Chen W, et al. Matrix metalloproteinases inhibition provides neuroprotection against hypoxia-ischemia in the developing brain. J Neurochem. 2009; 111:726–736. [PubMed: 19712057]

Coisne C, Engelhardt B. Tight junctions in brain barriers during central nervous system inflammation. Antioxid Redox Signal. 2011; 15:1285–1303. [PubMed: 21338320]

Deane R, et al. IgG-assisted age-dependent clearance of Alzheimer's amyloid beta peptide by the blood-brain barrier neonatal Fc receptor. J Neurosci. 2005; 25:11495–11503. [PubMed: 16354907]

Ek CJ, et al. Brain barrier properties and cerebral blood flow in neonatal mice exposed to cerebral hypoxia-ischemia. J Cereb Blood Flow Metab. 2015; 35:818–827. [PubMed: 25627141]

Fernandez-Lopez D, et al. Blood-brain barrier permeability is increased after acute adult stroke but not neonatal stroke in the rat. J Neurosci. 2012; 32:9588–9600. [PubMed: 22787045]

Gidday JM, et al. Leukocyte-derived matrix metalloproteinase-9 mediates blood-brain barrier breakdown and is proinflammatory after transient focal cerebral ischemia. Am J Physiol Heart Circ Physiol. 2005; 289:H558–H568. [PubMed: 15764676]

Hahn-Dantona E, et al. The low density lipoprotein receptor-related protein modulates levels of matrix metalloproteinase 9 (MMP-9) by mediating its cellular catabolism. J Biol Chem. 2001; 276:15498–15503. [PubMed: 11279011]

Hong SH, et al. Docosahexaenoic acid confers enduring neuroprotection in experimental stroke. J Neurol Sci. 2014; 338:135–141. [PubMed: 24433927]

Hong SH, et al. Docosahexaenoic acid improves behavior and attenuates blood-brain barrier injury induced by focal cerebral ischemia in rats. Exp Transl Stroke Med. 2015; 7:3. [PubMed: 25642315]

Jeffery RW, et al. Home testing of urine chloride to estimate dietary sodium intake: evaluation of feasibility and accuracy. Addict Behav. 1987; 12:17–21. [PubMed: 3565108]

Jin R, et al. Inflammatory mechanisms in ischemic stroke: role of inflammatory cells. J Leukoc Biol. 2010; 87:779–789. [PubMed: 20130219]

Krueger M, et al. Blood-brain barrier breakdown involves four distinct stages of vascular damage in various models of experimental focal cerebral ischemia. J Cereb Blood Flow Metab. 2015; 35:292–303. [PubMed: 25425076]

Labus J, et al. Interleukin-1beta induces an inflammatory response and the breakdown of the endothelial cell layer in an improved human THBMEC-based in vitro blood-brain barrier model. J Neurosci Methods. 2014; 228:35–45. [PubMed: 24631939]

Li P, et al. Adoptive regulatory T-cell therapy protects against cerebral ischemia. Ann Neurol. 2013a; 74:458–471. [PubMed: 23674483]

Li P, et al. Adoptive regulatory T-cell therapy preserves systemic immune homeostasis after cerebral ischemia. Stroke. 2013b; 44:3509–3515. [PubMed: 24092548]

Liuzzi GM, et al. Inhibitory effect of polyunsaturated fatty acids on MMP-9 release from microglial cells--implications for complementary multiple sclerosis treatment. Neurochem Res. 2007; 32:2184–2193. [PubMed: 17624613]

Maddahi A, et al. Enhanced cerebrovascular expression of matrix metalloproteinase-9 and tissue inhibitor of metalloproteinase-1 via the MEK/ERK pathway during cerebral ischemia in the rat. BMC Neurosci. 2009; 10:56. [PubMed: 19497125]

McColl BW, et al. Systemic inflammation alters the kinetics of cerebrovascular tight junction disruption after experimental stroke in mice. J Neurosci. 2008; 28:9451–9462. [PubMed: 18799677]

Moretti R, et al. Blood-brain barrier dysfunction in disorders of the developing brain. Front Neurosci. 2015; 9:40. [PubMed: 25741233]

Muramatsu K, et al. Vulnerability to cerebral hypoxic-ischemic insult in neonatal but not in adult rats is in parallel with disruption of the blood-brain barrier. Stroke. 1997; 28:2281–2288. discussion 2288-9. [PubMed: 9368577]

Neuhaus W, et al. The pivotal role of astrocytes in an in vitro stroke model of the blood-brain barrier. Front Cell Neurosci. 2014; 8:352. [PubMed: 25389390]

Petroni A, et al. Inhibition by n-3 fatty acids of arachidonic acid metabolism in a primary culture of astroglial cells. Neurochem Res. 1994; 19:1187–1193. [PubMed: 7824073]

Proulx DP, et al. Interaction between intravenous immunoglobulin (IVIg) and the low-density lipoprotein receptor-related protein 1: a role for transcytosis across the blood brain barrier? J Neuroimmunol. 2012; 251:39–44. [PubMed: 22796178]

Revuelta-Lopez E, et al. Hypoxia induces metalloproteinase-9 activation and human vascular smooth muscle cell migration through low-density lipoprotein receptor-related protein 1-mediated Pyk2 phosphorylation. Arterioscler Thromb Vasc Biol. 2013; 33:2877–2887. [PubMed: 24072693]

Rozanov DV, et al. The low density lipoprotein receptor-related protein LRP is regulated by membrane type-1 matrix metalloproteinase (MT1-MMP) proteolysis in malignant cells. J Biol Chem. 2004; 279:4260–4268. [PubMed: 14645246]

Shinto L, et al. Omega-3 fatty acid supplementation decreases matrix metalloproteinase-9 production in relapsing-remitting multiple sclerosis. Prostaglandins Leukot Essent Fatty Acids. 2009; 80:131–136. [PubMed: 19171471]

Shinto L, et al. The effects of omega-3 Fatty acids on matrix metalloproteinase-9 production and cell migration in human immune cells: implications for multiple sclerosis. Autoimmune Dis. 2011; 2011:134592. [PubMed: 21799946]

Song H, et al. Low-density lipoprotein receptor-related protein 1 promotes cancer cell migration and invasion by inducing the expression of matrix metalloproteinases 2 and 9. Cancer Res. 2009; 69:879–886. [PubMed: 19176371]

Srinivasakumar P, et al. Therapeutic hypothermia in neonatal hypoxic ischemic encephalopathy: electrographic seizures and magnetic resonance imaging evidence of injury. J Pediatr. 2013; 163:465–470. [PubMed: 23452588]

St-Pierre Y, et al. Emerging features in the regulation of MMP-9 gene expression for the development of novel molecular targets and therapeutic strategies. Curr Drug Targets Inflamm Allergy. 2003; 2:206–215. [PubMed: 14561155]

Svedin P, et al. Matrix metalloproteinase-9 gene knock-out protects the immature brain after cerebral hypoxia-ischemia. J Neurosci. 2007; 27:1511–1518. [PubMed: 17301159]

Wang J, et al. Omega-3 polyunsaturated fatty acids enhance cerebral angiogenesis and provide long-term protection after stroke. Neurobiol Dis. 2014; 68:91–103. [PubMed: 24794156]

Yang Y, Rosenberg GA. Matrix metalloproteinases as therapeutic targets for stroke. Brain Res. 2015

Yang Y, et al. Early inhibition of MMP activity in ischemic rat brain promotes expression of tight junction proteins and angiogenesis during recovery. J Cereb Blood Flow Metab. 2013; 33:1104–1114. [PubMed: 23571276]

Zhang M, et al. Omega-3 fatty acids protect the brain against ischemic injury by activating Nrf2 and upregulating heme oxygenase 1. J Neurosci. 2014; 34:1903–1915. [PubMed: 24478369]

Zhang W, et al. Omega-3 polyunsaturated fatty acid supplementation confers long-term neuroprotection against neonatal hypoxic-ischemic brain injury through anti-inflammatory actions. Stroke. 2010; 41:2341–2347. [PubMed: 20705927]

Zhang W, et al. Dietary supplementation with omega-3 polyunsaturated fatty acids robustly promotes neurovascular restorative dynamics and improves neurological functions after stroke. Exp Neurol. 2015; 272:170–180. [PubMed: 25771800]

Zhang Y, Pardridge WM. Mediated efflux of IgG molecules from brain to blood across the blood-brain barrier. J Neuroimmunol. 2001; 114:168–172. [PubMed: 11240028]

Zhao Y, Chen LH. Eicosapentaenoic acid prevents lipopolysaccharide-stimulated DNA binding of activator protein-1 and c-Jun N-terminal kinase activity. J Nutr Biochem. 2005; 16:78–84. [PubMed: 15681165]

Highlights

- Blood brain barrier was damaged after neonatal hypoxic-ischemic brain injury
- n-3 PUFA preserved the integrity of blood brain barrier following H/I
- n-3 PUFA alleviated degeneration of tight junction after neonatal H/I insult
- n-3 PUFA suppressed H/I induced activation of MMP-9 and MMP-2 both in brain and in blood

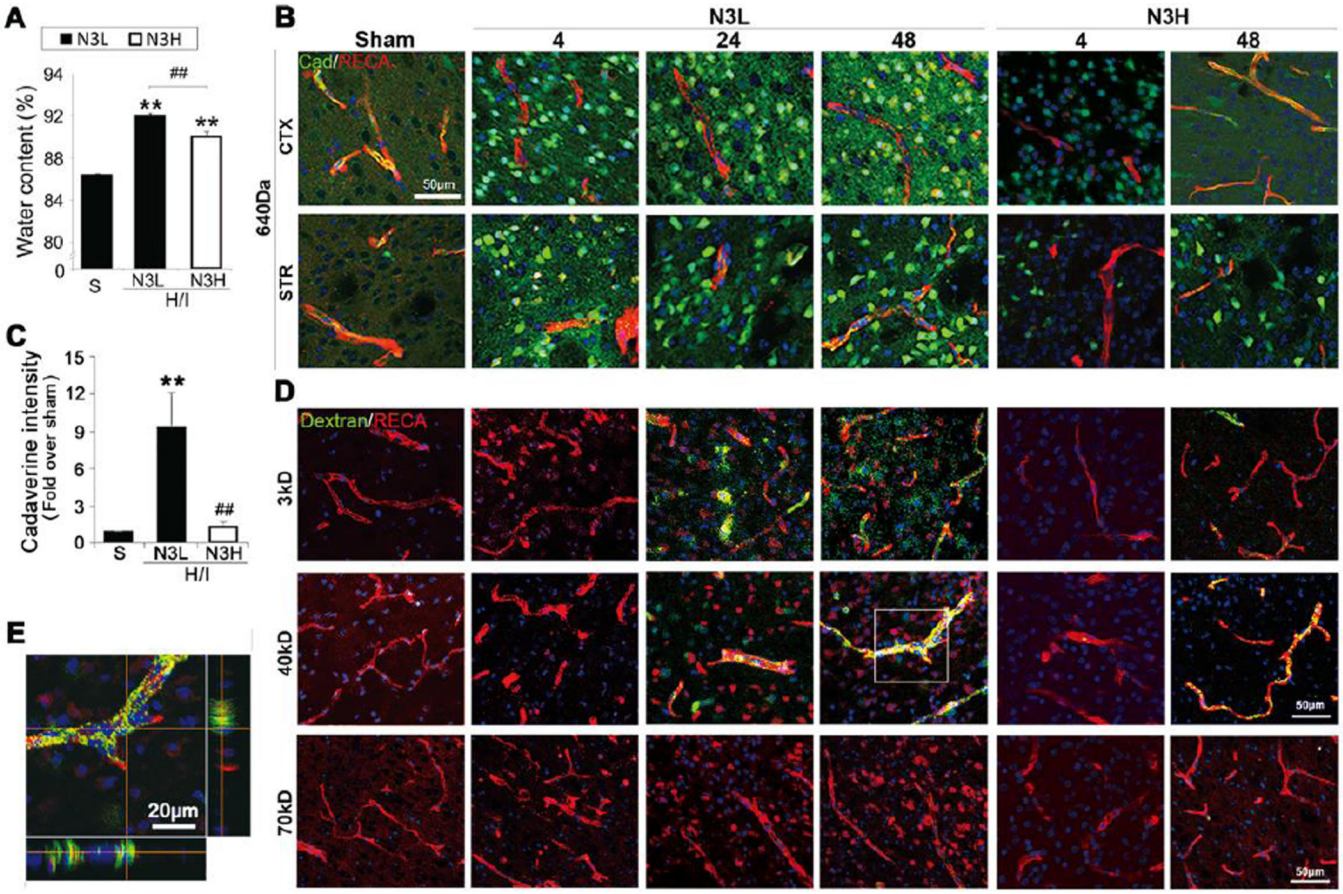

Figure 1.

n-3 PUFAs reduce extravasation of fluorescein-conjugated tracers with different molecular weights after H/I. (**A**) Quantification of brain water content after H/I (n=7 per group). (**B**) Intracranial extravasation of cadaverine-Alexa-488 at 4, 24 and 48 hours after H/I in cortex (CTX) and striatum (STR). (scale bar=50μm). (**C**) Quantification of cadaverine intensity at 48 hours after H/I. **p≤0.01 vs Sham, #p≤0.05 vs N3L H/I, Data are mean±s.d., n=6 per group. (**D**) Representative images of RECA and dextrans (3kD, 40kD and 70kD) after post-H/I intravenous injections at 4, 24 and 48 hours after H/I (scale bar=50μm). (**E**) Representative high magnification 3D view of 40kD dextran/RECA staining (enlarged image of inset in panel D) in N3L neonates at 48 hours after H/I (scale bar=20μm).

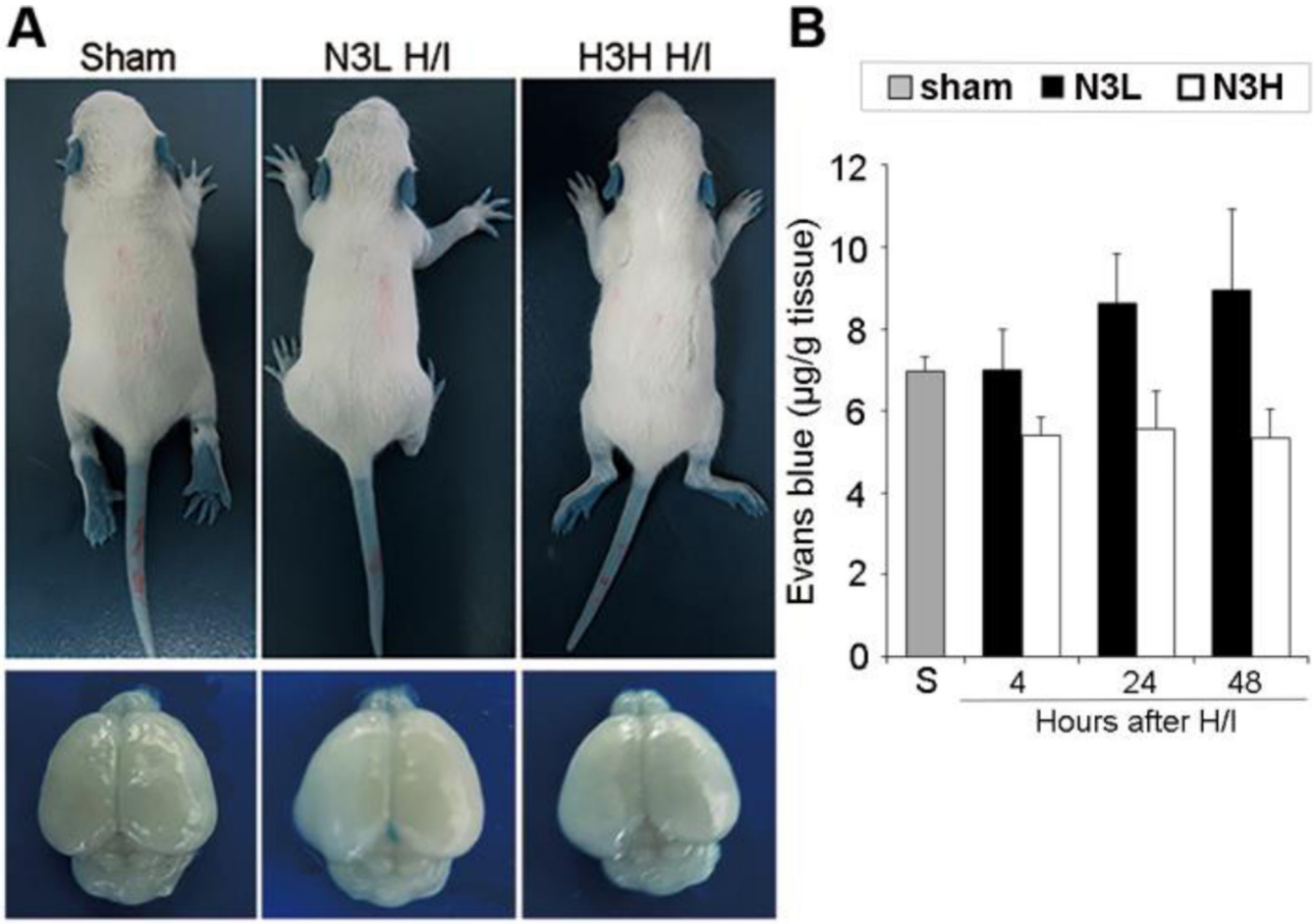

Figure 2.

Lack of intracranial extravasation of Evans blue after H/I injury in neonates. (**A**) Representative neonates (top) and whole brains (bottom) showing lack of Evans blue extravasation and accumulation in neonatal brains at 4, 24 and 48 hours after H/I. (**B**) Quantification of intravenously administered Evans blue in the brain at 4, 24 and 48 hours after H/I. Data are mean±s.d., n=5–7 pups per group.

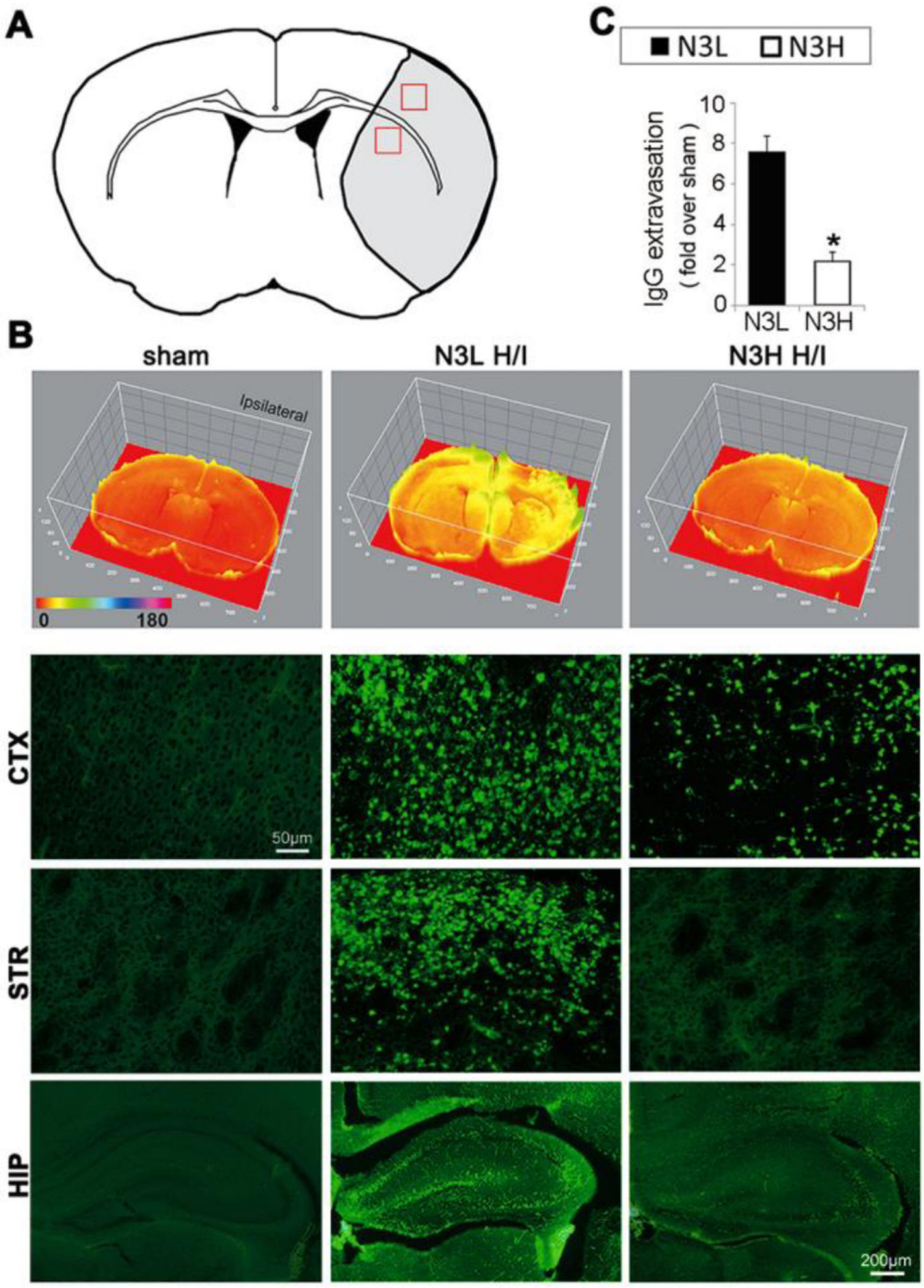

Figure 3.

n-3 PUFAs dramatically reduce extravasation of plasma-derived immunoglobulin G (IgG) at 48 hours after H/I. (**A**) The regions of interest for IgG measurements in cortex and striatum are marked by red squares. (**B**) Representative images of IgG expression using a 3D model (top panels) and immunostaining for rat IgG extravasation (lower panels) in cortex (CTX) and striatum (STR) (scale bar=50μm) and in hippocampus (scale bar=200μm) after H/I. (**C**) Quantification of IgG-positive area as determined by immunohistochemical staining. *p≤0.05 vs N3L H/I, data are mean±s.d., n=6 per group.

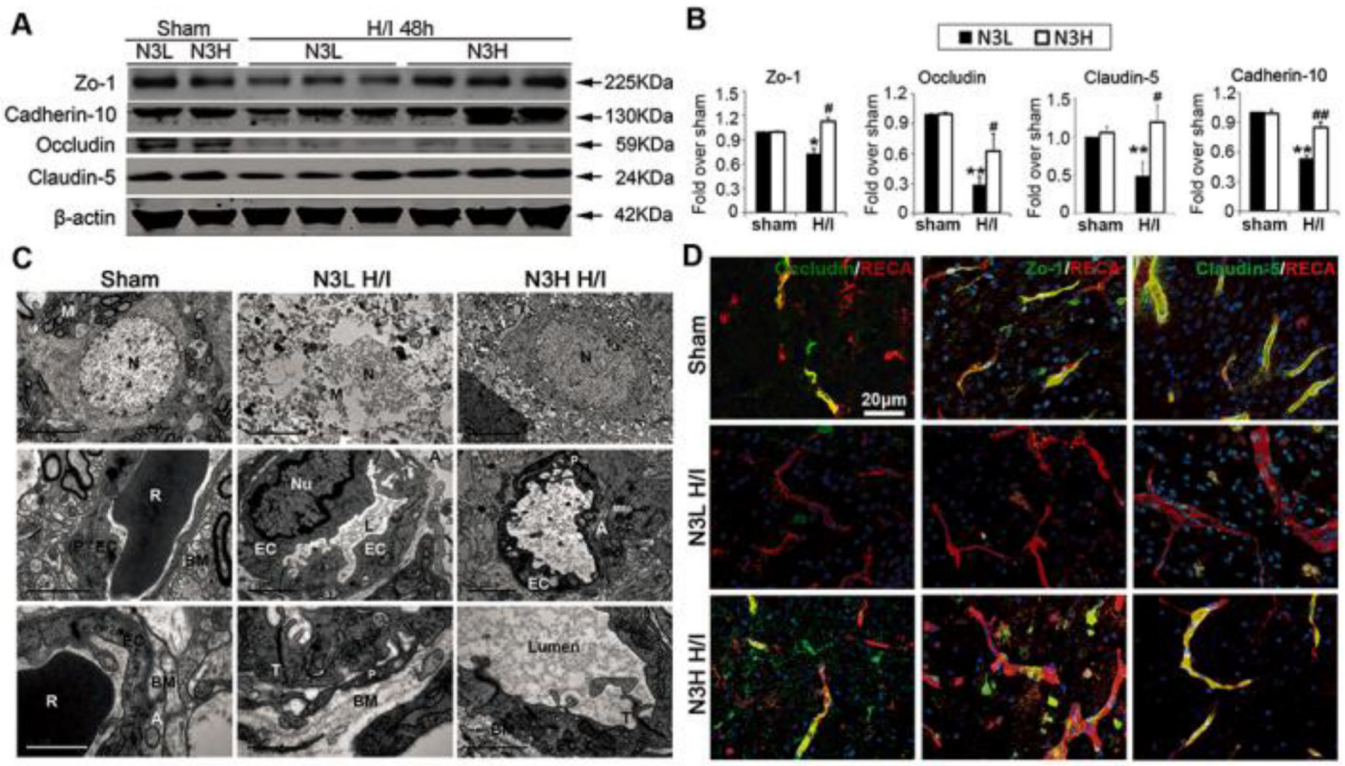

Figure 4.

n-3 PUFAs preserve the integrity of tight junctions after neonatal H/I. (**A**) Western blots showing expression of occludin, ZO-1, claudin-5, and cadherin-10 at 48 hours after H/I. (**B**) Quantification of occludin, ZO-1, claudin-5, and cadherin-10 levels at 48 hours after H/I. **p≤0.01,*p≤0.05 vs Sham, ##p≤0.01, #p≤0.05 vs N3L H/I, data are mean±s.d., n=6 each group. (**C**) Representative electron microscopic images of neuronal ultrastructure and the components of the BBB at 48 hours after H/I. N: neuron; P: pericyte, EC: endothelial cells; BM: base membranes; T: tight junction; Lumen: capillary lumen; R: a red cell; A: perivascular astrocytes; M: mitochondria. Scale bar: from top to bottom rows: 5μm, 2μm, and 1μm. (**D**) Representative immunofluorescent images of occludin, ZO-1, and claudin-5 with $RECA^+$ vessels and DAPI nuclear labeling at 48 hours following H/I brain injury (scale bar=20μm).

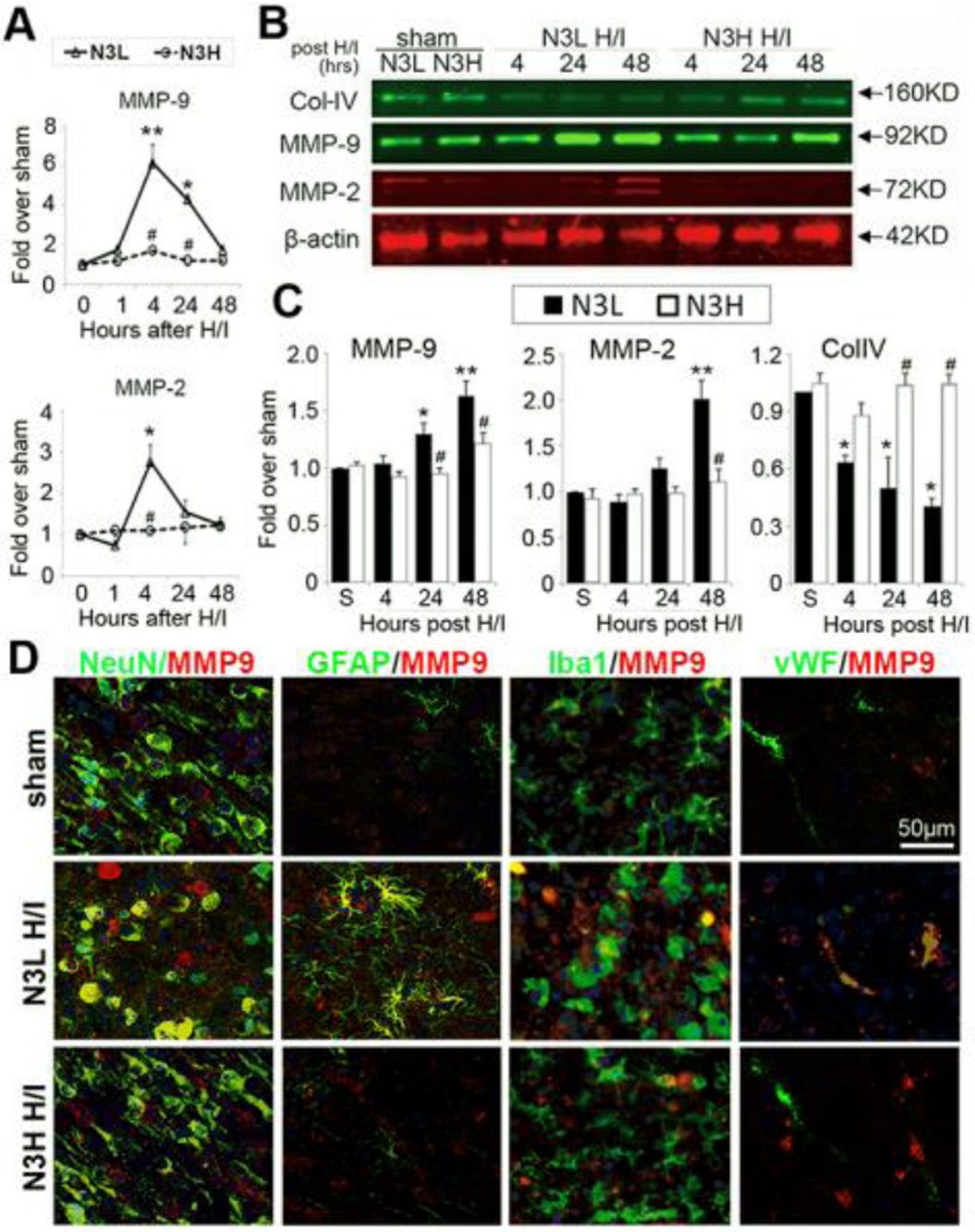

Figure 5.

n-3 PUFAs prevent the elevation of MMP-9 and MMP-2 in the brain and preserve Col-IV levels after neonatal H/I. (**A**) Quantification of MMP-2 and MMP-9 mRNA levels in the brain at 1, 4, 24, and 48 hours after neonatal H/I. (**B**) Western blots showing MMP-9, MMP-2, and Col-IV levels at 4, 24, and 48 hours after H/I. (**C**) Quantification of MMP-9, MMP-2, and Col-IV protein levels at the indicated time points after neonatal H/I. (**D**) Representative immunofluorescent images of MMP-9/NeuN, MMP-9/GFAP, MMP-9/Iba1,

and MMP-9/vWF at 48 hours after H/I. Nuclei were labeled with DAPI (scale bar=50μm). ** p≤0.01, *p≤0.05 vs Sham, # p≤0.05 vs N3L H/I, data are mean±s.d., n=6 each group.

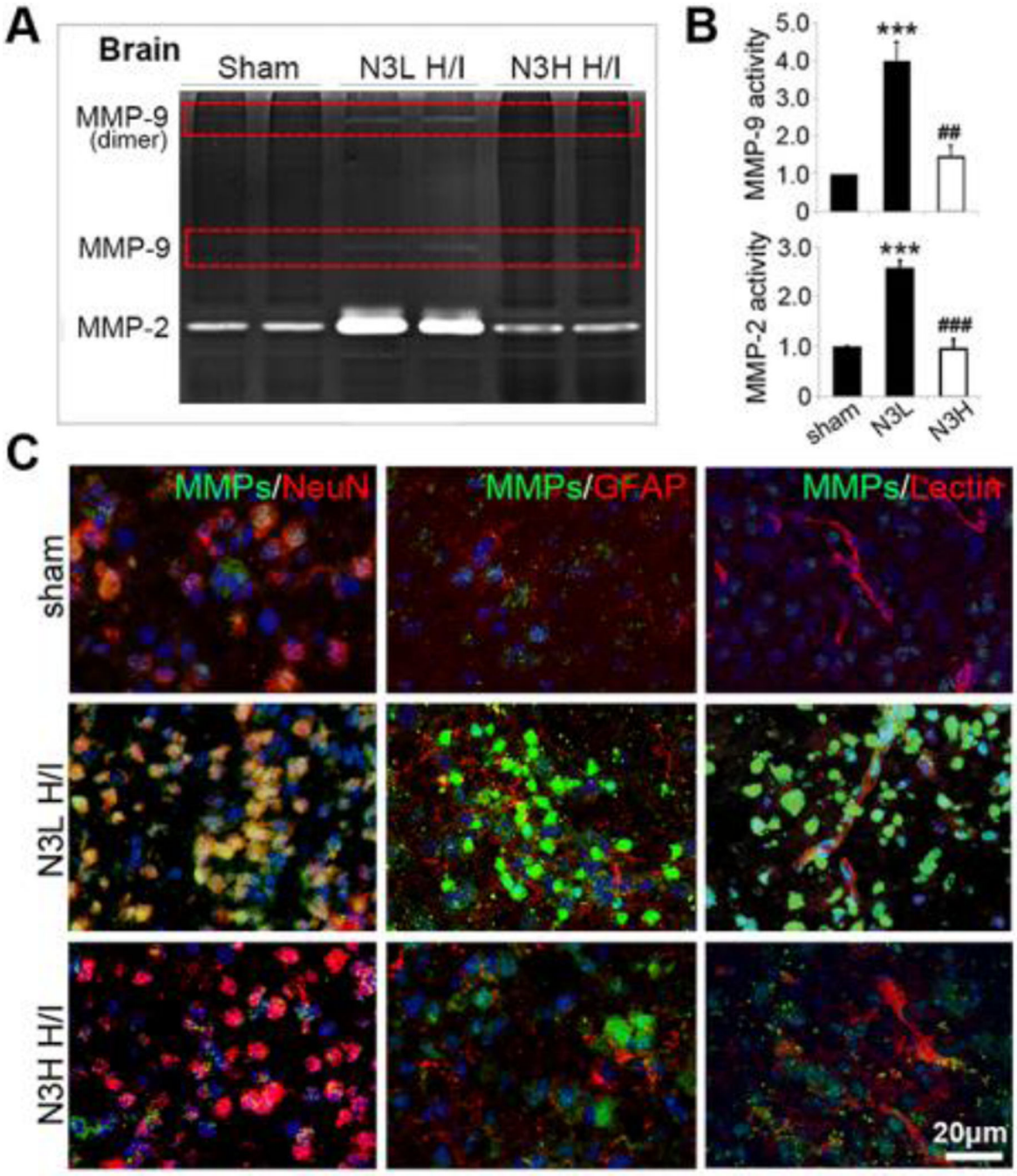

Figure 6.

n-3 PUFAs inhibit MMP activation after neonatal H/I. (**A**) Gelatin zymography shows MMP-9 and MMP-2 activity in brain tissue at 48 hours after H/I. (**B**) Quantification of MMP-9 and MMP-2 activity in the brain. (**C**) Representative immunofluorescent images of gelatinolytic activity (green) and NeuN, GFAP, and lectin (red) at 48 hours post H/I. Nuclei were stained with DAPI (blue; scale bar=20μm). **p≤0.01; ***p≤0.001 vs Sham, ##p≤0.01; ###p≤0.001 vs N3L H/I, data are mean± s.d., n=6 each group.